LA-UR- 01-5680



*Title:* MICROSTRUCTURAL DEVELOPMENT AND CONTROL IN YBa(2)Cu(3)O(y) COATED CONDUCTORS

*Author(s):*
Terry G. Holesinger, MST-6
Brady J. Gibbons, MST-STC
Steve R. Fol;tyn, MST-STC
Paul N. Arendt, MST-STC
J. Randy Groves, MST-STC
J. Yates Coulter, MST-STC

*Submitted to:* Volume 47 and 48 Advances in Cryogenic Engineering, proceedings of the joint CEC/ICMC Conference, Madison, WI
July 16-20, 2001

# MICROSTRUCTURAL DEVELOPMENT AND CONTROL IN $YBa_2Cu_3O_Y$ COATED CONDUCTORS.

T.G. Holesinger, B.J. Gibbons, S.R. Foltyn, P.N. Arendt, J.R. Groves, and J.Y. Coulter

Los Alamos National Laboratory
Los Alamos, NM 87545

## ABSTRACT

A study of some defect structures in $Y_1Ba_2Cu_3O_7$ (Y-123) coated conductors based on ion-beam-assisted-deposition (IBAD) of yttria-stabilized zirconia (YSZ) on nickel alloy substrates is presented. Defect structures can originate anywhere in the coated conductor architecture. Defects can be additive and propagate through the entire film structure to affect the growth, orientation, and properties of the superconducting film. Interfacial reactions between Y-123 and the underlying buffer layer and the corresponding effects on the transport properties of the films can be controlled with the thickness of the underlying buffer layer. With a 90Å ceria buffer layer on an IBAD YSZ coated metal substrate, a $J_c$ value of 1.7 MA/cm$^2$ (self-field, 75K) was obtained in a 1.5$\mu$m thick Y-123 film.

## INTRODUCTION

Ion-beam-assisted deposition (IBAD) is an effective method for preparing a biaxially-aligned template on polycrystalline metal substrates for subsequent oriented growth of oxide buffer layers and superconductors [1-3]. $YBa_2Cu_3O_y$ (Y-123) may be deposited directly onto the IBAD YSZ or MgO films. However, additional buffer layers such as $CeO_2$, are necessary for optimizing the transport properties and controlling defects in the Y-123 films[4,5]. The additional buffer layer(s) may provide a better lattice match to Y-123 [6] or improve the chemical stability of the interface relative to the high reactivity of barium in Y-123 [7].

Understanding the interactions between the Y-123 film, the underlying buffer layers, and the substrate is important for developing the IBAD process into a practical conductor technology. Each process used to deposit the bi-axially textured template, additional buffer layer(s), and the superconductor creates interfaces along which defects or interfacial reactions may result. These defects can be additive and propagate through the entire film structure to affect the growth and properties of the superconducting film. Defects within the films and at the interfaces can be structural, chemical, or a combination of both [4]. Their origins include substrate roughness, lattice mismatch, porosity, and interfacial reactions. $CeO_2$ is a stable oxide with a good lattice match to Y-123 and it has been successfully used as a buffer layer [3,8,9]. However, recent work has shown that even this

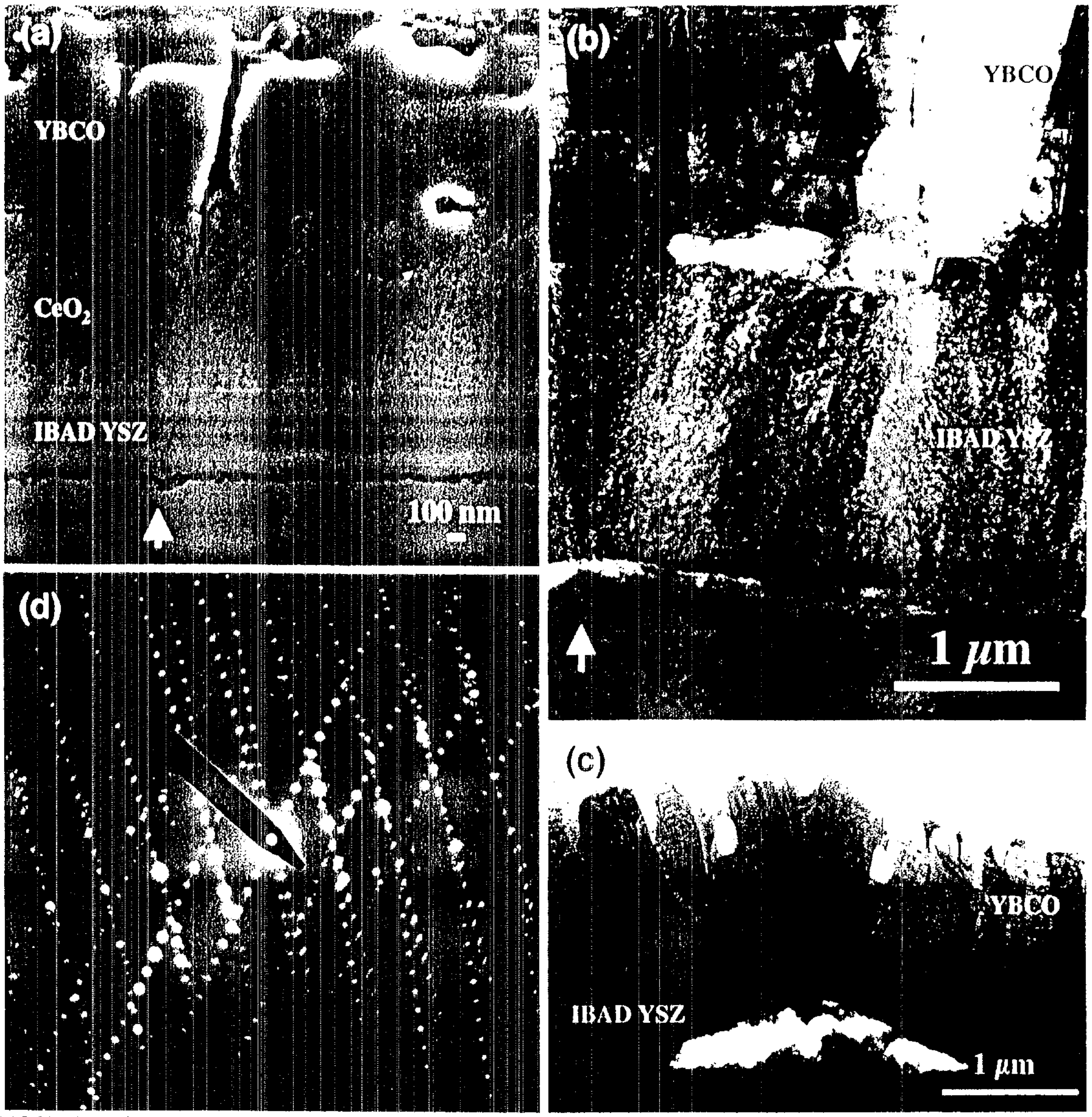


**FIGURE 1.** SEM , TEM, and SAD micrographs of types of substrate defects that thread through the buffer layers and affect Y-123 film growth. The SEM micrograph (a) shows the structure of a defect that starts at a pit in the substrate and ends as a pore in the Y-123 film. The TEM micrograph (b) shows the effect of a small hillock on the substrate and the ensuing disruption and discontinuity in the IBAD YSZ. Such discontinuities enhance interfacial reactions between the Y-123 and ceria. The TEM and SAD micrographs, (b) and (c) show the result of bubble formation between the substrate and YSZ. The growth of the Y-123 film over this defect results in a series of tilt boundaries between the Y-123 grains as indicated by the SAD micrograph (d).

highly stable material reacts with Y-123 along the interface and affects the superconductor's properties [4]. Since it appears that nearly all materials react with Y-123 at typical processing temperatures, it is especially important to understand what general aspects of the interfacial reactions between a given material and Y-123 limit or enhance the rate of reaction and what effects they may have on the transport properties.

## EXPERIMENTAL

IBAD was used to produce the biaxially-textured YSZ film on Inconel 625 or Hastelloy substrates. The ceria and Y-123 layers were deposited by pulsed laser deposition (PLD). The IBAD YSZ thickness was kept at 0.5 $\mu m$ while the thickness of the ceria and

Y-123 layers were varied between 5 and 1000 nm and 1 and 3 microns, respectively. Additional details of the deposition processes can be found elsewhere [10-12].

Transmission and scanning electron microscopy (TEM and SEM) samples were prepared in the same manner for viewing in the longitudinal transverse direction (perpendicular to both the nominal c-axis of the film and direction of current flow) [4]. Phase identification was performed by x-ray diffraction, energy dispersive spectroscopy (EDS) and electron diffraction.


**FIGURE 2.** TEM micrograph of a crack structure in the IBAD YSZ layer and the resulting reaction between the Y-123 and buffer layers that results in the formation of an extended defect.

## RESULTS

### Effects of Substrate Defects

Substrate and buffer layer defects can influence the growth of the Y-123 film. It has been found that the growth of the Y-123 film changes to accommodate these defects. These changes may be reflected in a change in alignment, generation of a structural defect in the Y-123 film, or the occurrence of an interfacial reaction phase. The SEM micrograph of FIG. 1a demonstrates how a substrate defect can propagate through the film and affect film growth. In this case, a large pore that spans the entire thickness of the film is formed. The sources of these substrate defects include surface roughness, cracks, pits or holes, bubble formation, and substrate inclusions. In general, no interfacial reactions are found between the IBAD YSZ and metal substrate. The layer that forms between them is the passivating $Cr_2O_3$ layer that normally forms on Ni-Cr alloys that are exposed to oxygen at elevated temperatures as occurs during Y-123 deposition.

The fine structure of these defects is shown in the TEM and SAD micrographs of FIG. 1b, c, and d. In FIG. 1b, the local alignment of the IBAD YSZ layer changes such that an imprint of the substrate defect is transferred through the subsequent layers. The end result is an area of enhanced reactivity at the ceria / Y-123 interface. Inclusions and delaminations at the metal/buffer interface can lead to the microstructure shown in FIG 1c. The presence of the bubble before Y-123 deposition is indicated by the dense film and alignment of the Y-123 to accommodate the defect. The result, as indicated by the diffraction pattern in FIG. 1d, is a series of a relatively high-angle tilt boundaries in the Y-123 film.

Little reaction occurs between the interior buffer layers. However, the morphology of the interfaces will follow the underlying substrate. Problems occur when cracks develop in the buffer layers and reach the Y-123 film. These defects greatly enhance interfacial reactions. Transport of material from the Y-123 film into the underlying buffer layers and substrate and vice-versa occurs as shown in FIG 2.

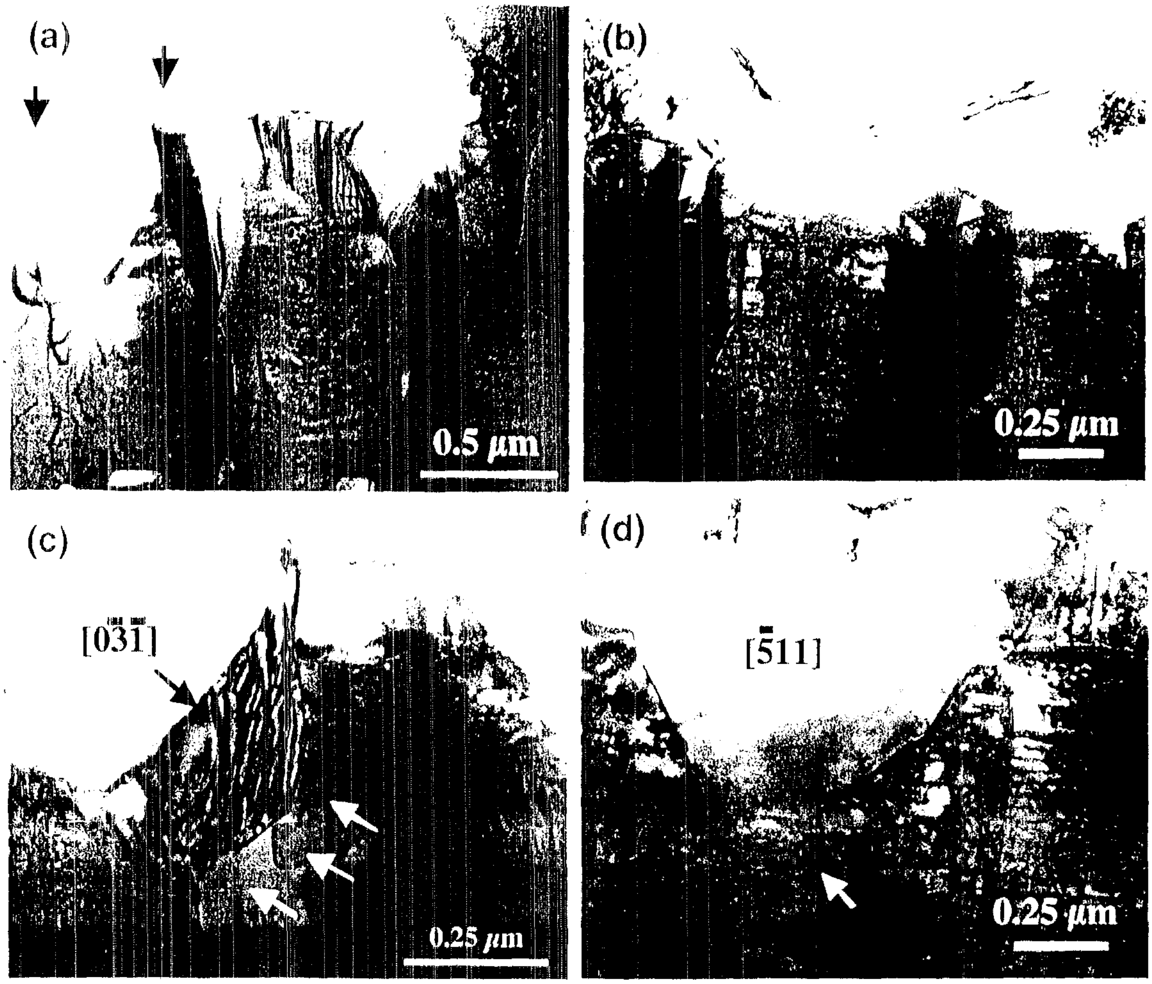


FIGURE 3. TEM micrographs of misoriented grains in the Y-123 films. Typical orientations are (a) a-axis, (b) 45° in-plane rotated, and (c) tilted Y-123 grains. The indicated orientations in (c) and (d) are approximately parallel to the [110] direction in the film. The tilted grains are not coherent with the film matrix and appear to be randomly oriented around the [001] direction.

## Misaligned Grains in Y-123 Films

Misalignments in the Y-123 film of the coated conductor can take the form of a-axis, 45° in-plane rotated, and tilted grains. Examples are shown in FIG. 3. A-axis oriented grains are often found in films deposited under non-optimal conditions. Grains rotated 45° in-plane have also been found in the Y-123 films as shown in FIG. 3b. No specific causes for their appearance have yet been clearly identified. The last example is of grains that are tilted as shown in FIG. 3c and d. These grains have an inverted, pyramidal shape. Once nucleated, these grains tend to grow faster than the matrix and often protrude above the nominal film surface. Randomly oriented interfacial reaction products are a cause for their nucleation in the film. The inverted pyramidal shape for the latter class of misoriented grains suggests a role as a potential current limiting defect having a thickness dependence.

## $CeO_2$ Thickness Effects

The Y-123 film properties and interfacial reactions at the Y-123 / ceria interface can be controlled by a suitable choice for thickness of the underlying buffer material (ceria). Shown in FIG 4 is a plot of the critical current density ($J_c$) as a function ceria thickness for Y-123 films deposited on IBAD YSZ-coated metal substrates. This maximum in $J_c$ correlates with a minimum in the reactivity between the ceria buffer layer and Y-123 film.

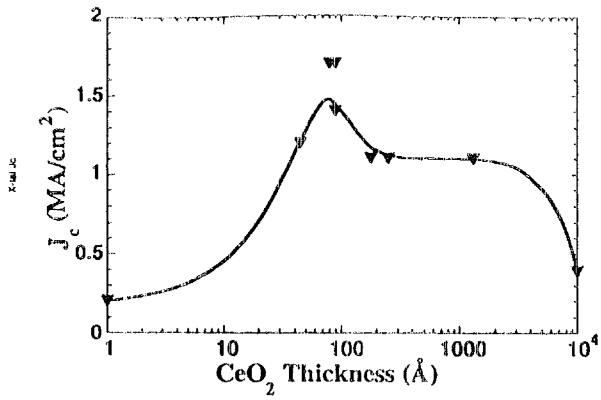


FIGURE 4. Plot of $J_c$ versus the thickness of the ceria buffer layer next to the Y-123 film. The Y-123 films were approximately 1.5 $\mu$m thick and the critical thickness of the $CeO_2$ layer was ≈ 90Å.

The critical ceria layer thickness on the IBAD YSZ metal tapes was approximately 90Å. The maximum $J_c$ value reached with a 90Å ceria film and a 1.5$\mu$m Y-123 film was 1.7 MA/cm$^2$ at 75K and self-field. At the critical thickness, the interfacial reactions were found to be almost non-existent as shown in FIG. 5a. The few that were found could be traced to the propagation of non-uniformities in the substrate to the ceria/Y-123 interface as shown in FIG. 6. $J_c$ decreases and interfacial reactions increase as the ceria buffer layer thickness moves away from the optimal value. FIG. 5b shows the interface in a film where the ceria thickness was initially 1000Å. Large portions of the interface have reacted to form $BaCeO_3$ and $YCuO_2$ [4]. The reactions between the ceria and Y-123 tend to stop when the underlying IBAD YSZ/ceria interface is reached. Conversely, the extension of the reaction products into the Y-123 increases without bound as the severity of the interfacial reactions increase. The reaction products also serve as nucleation sites for misaligned Y-123 grains as shown above. These results suggest that interfacial reactions play a significant role in forming current limiting defects in Y-123 films.

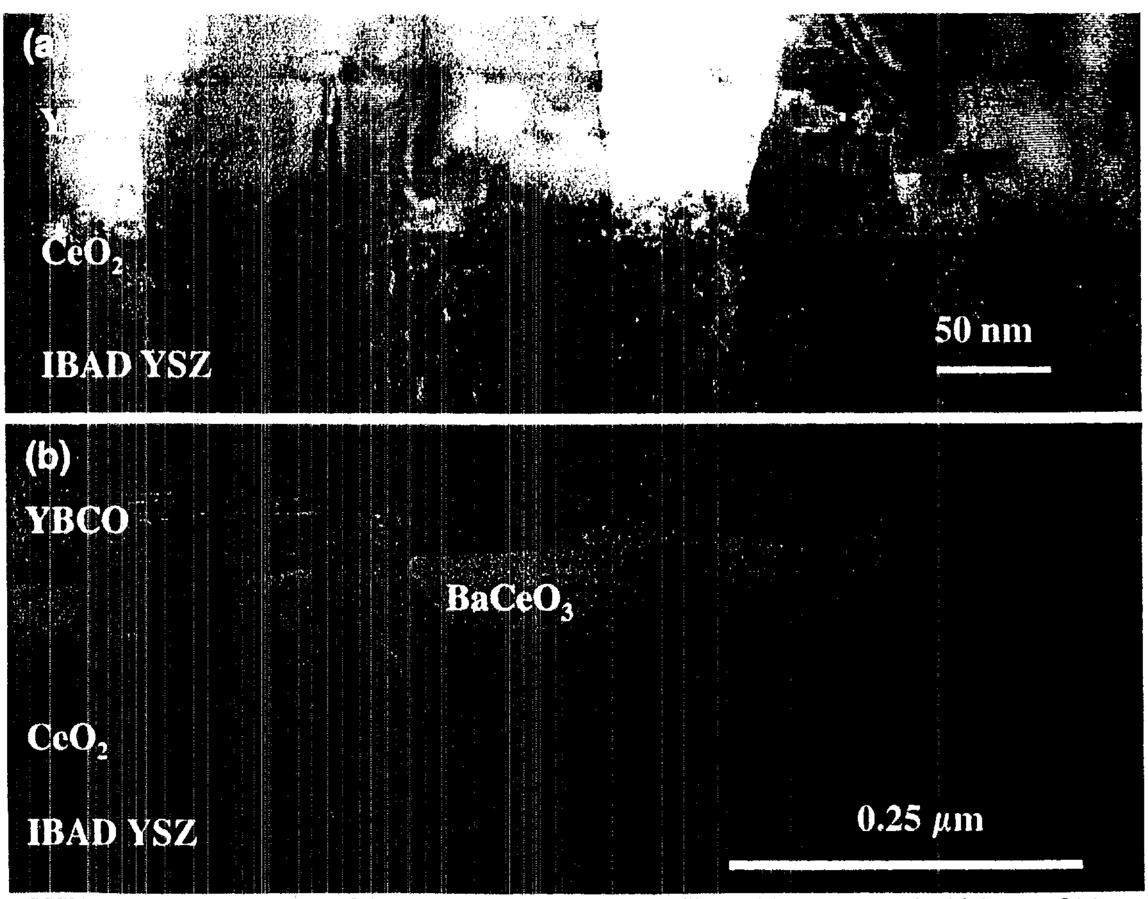


FIGURE 5. TEM micrographs of the Y-123 / ceria interfaces in films with nominal ceria thickness of (a) 90Å and (b) 1300Å. Whereas in (a) no interfacial reactions are found, a nearly continuous layer of $BaCeO_3$ is present in (b).

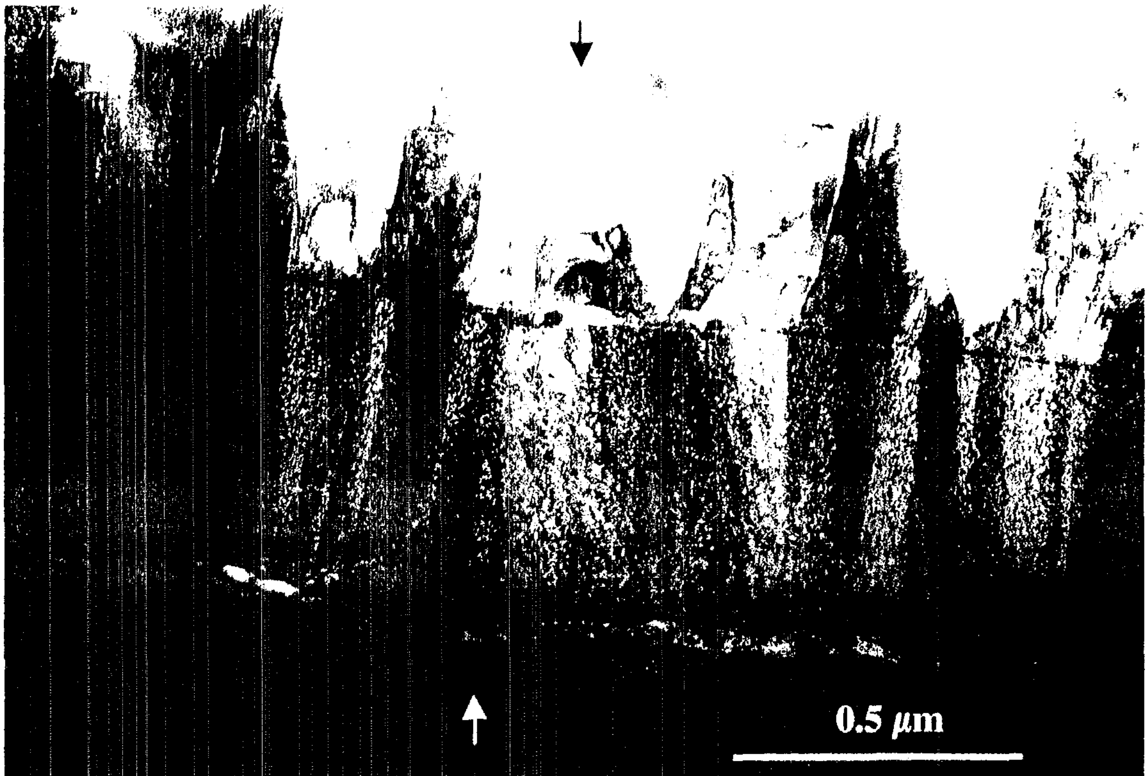


**FIGURE 6.** TEM micrograph of a Y-123 coated conductor. The ceria thickness was 90Å which minimized the interfacial reactions. The only interfacial reactions present in this sample where those caused by substrate defects that propagate through the buffer layers as shown above. The resulting discontinuity in the substrate leads to an interfacial reaction at the Y-123 / ceria interface and a large pore in the Y-123 film.

## DISCUSSION

Maximizing the $J_c$ properties of the Y-123 coated conductors requires an understanding the origin of current limiting defects. A prime area for concern is the preparation of the substrate surface prior to film deposition. The results show that any defects in the substrate transfer through the buffer layers to adversely affect the growth of the Y-123 film due to changes in morphology or chemical reactivity. In addition to the role it plays for biaxial alignment, the IBAD YSZ layer is also a diffusion barrier [13]. Defects such as cracks in the buffer layers defeat this purpose as they are chemically more reactive and allow transport of material from the film into the underlying buffers and substrate and vice-versa.

Misoriented grains within the film are also a concern for maximizing $J_c$. Their origins are varied and their presence can be used as guide to determining optimal deposition conditions or gauging the extent of interfacial reactions. The presence of the a-axis grains can be used to address the former point while a measure of the tilted Y-123 grains can be a gauge of the latter. Many of the tilted Y-123 grains could be traced to nucleation on a randomly oriented interfacial reaction phase such as CuO, $YCuO_2$, or $BaCeO_3$. Other deleterious effects of the reactions are intergrowths within the Y-123 gains [4]. Hence, it is very advantageous that the interfacial reactions can be minimized through a suitable choice of the final buffer layer thickness. For the case of ceria on IBAD YSZ, the critical thickness was around 90Å. The $J_c$ value of 1.7 MA/cm$^2$ is one of the highest values measured for Y-123 films greater than 1 μm in thickness on polycrystalline metal substrates. Further increases in the $J_c$ performance will come with the mitigation of substrate defects like the one shown in FIG 6.

## SUMMARY

The origin of some defect structures in Y-123 coated conductors based on the IBAD process was examined. The defects can be additive and propagate through the entire film structure to affect the growth, orientation, and properties of the superconducting film. The interfacial reactions and the transport properties of the Y-123 films can be controlled by a careful choice of the thickness of the underlying buffer layer. In the case of a ceria buffer layer, a critical thickness value of 90 Å was found for which the interfacial reactions were minimized. A record $J_c$ value of 1.7 $MA/cm^2$ (self-field, 75K) was obtained in a 1.5$\mu$m thick Y-123 film on an IBAD YSZ / metal substrate with an intervening 90Å ceria buffer layer. Further increases above this level of performance will come with the elimination of substrate-induced defects.

## ACKNOWLEDGEMENTS

This work was performed under the auspices of the United States Department of Energy, Office of Energy Efficiency and Renewable Energy, as part of a DOE program to develop electric power technology, under contract W-7405-ENG-36.

## REFERENCES

1. Y. Iijima, N Tanabe, O. Kohno et al., *Applied Physics Letters* **60** (6), 769-771 (1992).
2. R.P. Reade, P. Berdahl, R.E. Russo et al., *Applied Physics Letters* **61** (18), 2231-2233 (1992).
3. X.D. Wu, S.R. Foltyn, P. Arendt et al., *Applied Physics Letters* **65** (15), 1961-1963 (1994).
4. T.G. Holesinger, S.R. Foltyn, P.N. Arendt et al., *Journal of Materials Research* **15** (5), 222-240 (2000).
5. T.G. Holesinger, S.R. Foltyn, P.N. Arendt et al., *IEEE Transactions on Applied Superconductivity* **11** (1), 3359-3364 (2001).
6. X.D. Wu, S.R. Foltyn, P.N. Arendt et al., *Applied Physics Letters* **67** (16), 2397-2399 (1995).
7. C.T. Cheung and E. Ruckenstein, *Journal of Materials Research* **4** (1), 1-15 (1989).
8. X.D. Wu, R.C. Dye, R.E. Muenchausen et al., *Applied Physics Letters* **58** (19), 2165-2167 (1991).
9. P. Merchant, R.D. Jacowitz, K. Tibbs et al., *Applied Physics Letters* **60** (6), 763-765 (1992).
10. P.N. Arendt, S.R. Foltyn, J.R. Groves et al., *Applied Superconductivity* **4** (10-11), 429-434 (1996).
11. S.R. Foltyn, P. Tiwari, R.C. Dye et al., *Applied Physics Letters* **63** (13), 1848-1850 (1993).
12. S.R. Foltyn, P.N. Arendt, P.C. Dowden et al., *IEEE Transactions on Applied Superconductivity* **9** (2), 1519-1522 (1999).
13. R.P. Reade, X.L. Mao, and R.E. Russo, *Applied Physics Letters* **59** (6), 739-741 (1991).